A Study of Helicopter Rotor Rotational Noise

A. Lee,* W. L. Harris,† and S. E. Widnall‡
Massachusetts Institute of Technology, Cambridge, Mass.

The rotational noise of model helicopter rotors in forward flight was studied in an anechoic wind tunnel. The parameters under study were the rotor thrust (blade loading), blade number, and advance ratio. The separate effects of each parameter were identified with the other parameters being held constant. The directivity of the noise was also measured. Twelve sets of data for rotational noise as a function of frequency were compared with the theory of Lowson and Ollerhead. In general, the agreement is reasonably good, except for the cases of 1) low and high disk loadings, 2) the four-bladed rotor, and 3) low advance ratios. The theory always underestimates the rotational noise at high harmonics.

I. Introduction

FOR a typical helicopter, aerodynamic noise is produced by the main rotor, the tail rotor, and the engine. At large distances from the vehicle, the low-frequency noise from the main rotor dominates since the higher frequencies are absorbed by the atmosphere.

According to Cox,[1] the aerodynamic noise from main rotors can be classified into two main categories: rotational (harmonic) noise and broadband noise. The aerodynamic sources of rotational noise are mean lift and drag forces, harmonic force fluctuations, and blade thickness. The sources of broadband noise are random force fluctuations and wake self-noise.

A prominent and impulsive sound occurs when a helicopter operates in certain conditions. This impulsive noise, blade slap, belongs to the rotational noise category, but it is usually distinguished as a separated noise source. In this paper, only the rotational noise of a low-speed rotor is under study. The rotor is in steady flight condition without the occurrence of impulsive noise.

In his classic paper, Gutin[2] identified the rotating steady forces (thrust and drag) as the source of propeller noise. Gutin's propeller noise theory systematically underestimated the noise level of higher harmonics in predicting the helicopter rotor noise. The fundamental frequency for a helicopter rotor is normally below the range of hearing so that it is only the higher harmonics which are important as a noise source. The first work to include the unsteady load components in rotor noise study was that of Schlegel et al.[3,4] Shortly thereafter, Lowson and Ollerhead,[5] Sadler and Loewy,[6] and Wright[7,8] in their parallel works gave analytic solutions for the rotational noise. In these analyses,[3-8] only the unsteady force fluctuations that act over the rotor disk were considered. These analyses are, therefore, valid up to high Mach number where compressibility effects will enhance the importance of thickness.

The theoretical noise-prediction models require a knowledge of the unsteady loading in the higher modes. Unfortunately, the information on the required unsteady loading, typically above the 30th harmonic of the blade passage frequency, is not available. At this point, most helicopter noise theories employ existing experimental data to develop semiempirical prediction schemes. Lowson and Ollerhead[5] studied the experimental data on the first ten harmonics of the fluctuating airloads measured by Scheiman.[9] Reference 5 assumed an inverse power law for the harmonic loading amplitude. Furthermore, the phase angles between loading harmonics are assumed to be random, and a nondimensional spanwise correlation length inversely proportional to the loading harmonic number is assumed to correlate the harmonic loads over the blade span. Although these assumptions inevitably result in some errors, Ref. 5 is a relatively efficient and accurate method to predict helicopter rotor noise. However, the lack of accurate and reliable helicopter noise data, especially in forward flight, has prevented the thorough evaluation of the theories, and, therefore, hindered the understanding of noise mechanisms and the development of reliable prediction methods.

The most complete data on rotor noise are obtained from whirl tower tests, which, of course, do not simulate high-speed forward flight. Up to this time, the experimental data of rotor noise in forward flight has been obtained largely from flight tests. In addition to the contaminations and uncertainties on the data measured in fly-overs, it is impossible for a helicopter to vary one parameter over a wide range with all other parameters unchanged and still maintain steady flight. Recently, an in-flight technique for measuring helicopter noise by stationkeeping with a quiet instrumented lead aircraft was developed.[10] This technique is very successful in measuring main rotor impulsive noise, but some difficulties in separating the effect of one parameter from the others on noise radiation still exist.

One obvious solution to these problems is proper simulation of forward flight in a wind tunnel. Cox[11] obtained some rotor noise data in the hard-walled 40×80-ft wind tunnel at the NASA Ames Research Center. Due to tunnel noise and wall reflections, the rotational noise data are difficult to interpret. Those results, however, are useful for the study of the impulsive noise and for assessing the effect of rotor design changes. Bauer and Widnall[12] developed a V/STOL noise facility consisting of an open jet tunnel operating within an anechoic chamber. Further extensive development and calibration have been done to ensure accurate reproduction of the essential features of both the aerodynamics and acoustics of the rotor system.[13] The rotational noise data presented in this paper were obtained in this facility. The effects of individual parameters on rotational noise were studied with all other parameters constant. The parameters studied include thrust, blade number, and advance ratio. Twelve sets of experimental data for rotational noise as a function of frequency have been

Presented as Paper 76-564 at the 3rd AIAA Aero-Acoustics Conference, Palo Alto, Calif., July 20-23, 1976; submitted Aug. 5, 1976; revision received April 25, 1977.

Index categories: Helicopters; Noise.

*Research Associate, Department of Aeronautics and Astronautics; now Senior Research Engineer, Beam Engineering, Inc., Sunnyvale, California. Member AIAA.

†Associate Professor, Department of Aeronautics and Astronautics. Member AIAA.

‡Professor, Department of Aeronautics and Astronautics. Member AIAA.

compared with the theoretical prediction of Lowson and Ollerhead.[5] The directivity of noise harmonics was measured and shows a consistent pattern with theory.

II. Experimental Apparatus

The wind tunnel was a 5-×7.5-ft (1.52- ×2.29-m) open jet test section enclosed within a 10-×11-×30-ft (3.05-×3.35-×9.14-m) anechoic chamber. The acoustic properties of the test section were calibrated by using white noise sources at various points in the test section. A typical anechoic property of the chamber is shown in Fig. 1. The lowest frequency (cut-off frequency) above which the freefield condition is obtained is 160 Hz. The effect of the open jet shear layer on sound transmitting through was studied by using Aeolian tones as the sound source, and was found to be insignificant within the conditions of our experiment. More detailed aerodynamic and acoustic calibrations on this facility may be obtained in Ref. 13.

A 4.17-ft (1.27-m) diam model rotor with flapping hinge was used in this study. The characteristics of this rotor are summarized in Table 1.

A dynamometer was designed to mount on top of the rotor shaft. Standard temperature-compensated semiconductor strain gage bridges and slip ring technology was applied in the design. The dynamometer is capable of measuring steady rotor thrust and unsteady rotor thrust up to 300 Hz. The thrust of 0.1 lb (0.05 kg) can be measured without difficulty. (The sensitivity was 0.577 mV/lb (1.27 mV/kg) with 6-V dc excitation voltage.) No hysteresis or temperature effect on the calibration was found throughout the operating range. The rotor hub, which floats on two sets of flexures inside the dynamometer, can take any number of blades from two to eight.

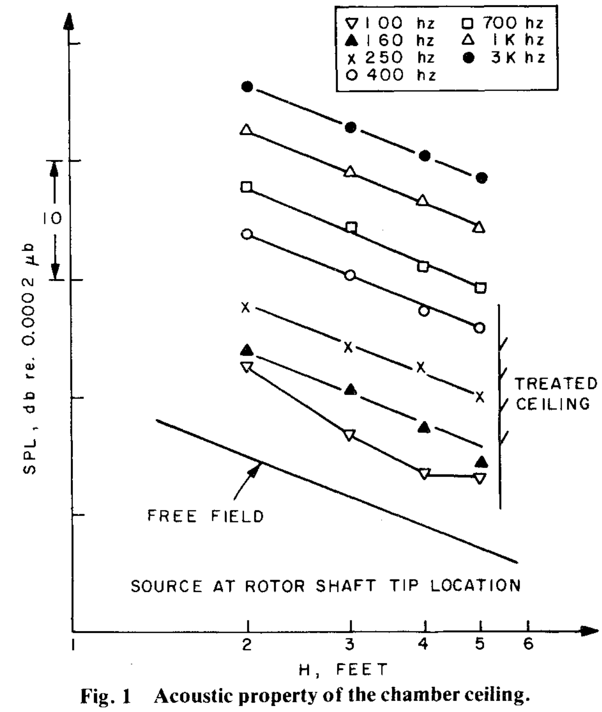

Fig. 1 Acoustic property of the chamber ceiling.

Table 1 Model rotor characteristics

Radius (R)	25 in. (0.635 m)
Chord (C)	2 in. (5.08 cm)
Number of blades	2, 3, 4, 6
Section	NACA 0.0012
Twist	−8 deg
Shaft tilt capability	±20 deg
Maximum rpm	1200
Testing rpm	672, 1100
Lead-lag	none
Cyclic pitch	none
Collective pitch	by adjusting the pitch of each blade

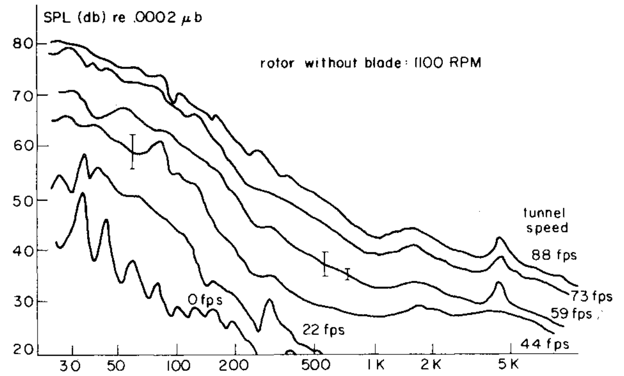

Fig. 2 Hz-constant band background noise of tunnel-rotor system.

Figure 2 shows a 1-Hz constant band background noise of the model rotor system running without blades at 1100 rpm with various tunnel speeds. In general, the background noise of the system (tunnel plus rotor) is below the measured rotor noise for frequencies above 200 Hz when the rotor speed is 1100 rpm. For the rotor speed of 672 rpm, the background noise and rotor noise are about the same level. Proper data processing was required to obtain valid rotor noise data.

III. Instrumentation and Data Processing Techniques

The acoustic signal was measured using a 0.5-in. Bruel and Kjaer (B&K) condenser microphone type 4133 with cathode follower type 2614. The microphone was calibrated with a B&K pistonphone type 4220. The rotor noise data were processed by applying a periodic sampling technique. This technique involves the use of a PAR Waveform Eductor, Model TDH-9. The waveform eductor samples the repetitive input and stores them in a 100-channel capacitance memory. After a sufficient number of sweeps (which is proportional to the characteristic time constant) have occurred, noise and other nonrepetitive signals will be suppressed since their average value will approach zero. The processed rotor noise data will contain only the rotational noise. The waveform eductor must be synchronized with the waveform of the signal; the time relationship between any point on the waveform and triggering must be constant. The 1/rev pulse generated by a photo tachometer was used for triggering. The variation of the triggering pulse was found to be within ±0.33%. This corresponds to an error of ±1.2 in 360 deg. This small error did not affect the accuracy of the data process. The acoustic data were analyzed on-line and off-line.

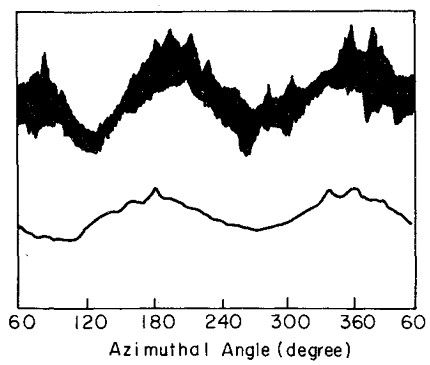

Fig. 3 Waveform of rotor noise signal: top trace – raw signal, bottom trace – averaged signal, tunnel speed = 59 fps (18.0 m/s), rotor speed = 1100 rpm, blade pitch at tip = 5 deg, shaft angle = 10 deg tilt forward.

For off-line analysis, both the acoustic signal and the triggering pulse were recorded simultaneously on a magnetic tape; each voltage signal occupied a track. Figure 3 shows a typical rotor noise waveform before and after processing. The top trace is the raw signal and the bottom trace is the averaged signal.

The harmonic content of the averaged acoustic signal was obtained by applying real-time analysis that gave ultra-narrow band (1 Hz) spectra at a much faster rate. A Federal Scientific Ubiquitous Spectrum Analyzer Model UA-15A and a Spectrum Averager Model 1015 were used to obtain the rotational noise content up to 500 Hz. As is well known, the use of a finite number of data channels (100 in the waveform eductor) results in a loss of resolution and spectrum folding at frequencies higher than the Nyquist frequency, $f_s = (\frac{1}{2}h)$, where h is the time increment of each channel. In these tests, the rotor angular velocity is 672 rpm, which results in a Nyquist frequency of 560 Hz (higher than the 500-Hz limit of the test.)

IV. Rotational Noise in Forward Flight

There are many parameters that influence rotational noise. To study the effect of one parameter on noise radiation, the other parameters should be kept constant. The parameters studied in this investigation are thrust, blade number, and advance ratio. The test conditions are listed in Table 2. The acoustic data were measured 53 in. (1.35 m) above the rotor, along the rotor tip path plane axis. The rotor thrust was measured with the dynamometer system and read out from a digital voltmeter, within an accuracy of $\pm 6.2\%$. The tip path plane was measured from the photographs taken in the tests. In order to maintain a constant tip path plane (in addition to a constant thrust in the study of blade number effect and advance ratio effect), the blade pitch and shaft angle must be adjusted together. The initial rotor settings were based on the rotor performance calculation. The proper settings were then obtained by iteration. In general, no more than three iterations were required to obtain proper settings in each test run.

The experimental acoustic data were compared with the theoretic predictions of Lowson and Ollerhead.[5] In their theory, the unsteady force fluctuations over the rotor disk are Fourier-analyzed into a series of modes. The coefficient of each mode of acoustic radiation is then determined by weighted integrals of the unsteady force fluctuations over the rotor disk, based on standard acoustic theory. The theoretical noise predictions require a knowledge of the higher modes of the unsteady loading, which is not available either experimentally or theoretically. Lowson and Ollerhead[5] examined the first ten harmonics due to airloading of helicopter rotors as measured in flight.[9] An inverse power relation was found to fit these data approximately. The λth harmonic loading amplitude F_λ was assumed to decay as $F_\lambda = F_0 \lambda^{-k}$, where F_0 is the steady loading, and k is a constant whose value is determined by the best fit of airloading data. For normal flight conditions, a value of $k=2$ was chosen. The λ^{-2} relation was applied to the whole frequency range, although it was obtained based on the correlation of low-harmonic data.

In addition to the amplitude, the effect of the phase relation between the loading harmonic is important in noise radiation. Since there are no useful data available, the phase relation between the loading harmonics is assumed to be completely random. The airloads are distributed over the blade, and the phase correlation along the span must be defined. The nondimensional spanwise correlation length was assumed to be inversely proportional to λ. The correlation coefficient can therefore be written as $e^{-a\lambda\xi}$, where ξ is the nondimensional distance between any two points along the span. The value of correlation parameter a is a function of flight conditions. A value of 8/3 was arbitrarily chosen. An effective point loading was then determined to represent the distributed loading along the span of the blade. Furthermore, a delta function representation was used for the chordwise loading distribution.

Based on the above assumptions, Lowson and Ollerhead[5] were able to predict the rotational noise radiation. As a result of the required complicated numerical calculations, a set of design charts were prepared for accurate and quick usage. They claimed that calculations based on these charts would yield the rotational noise harmonics, at any point in the far field of the rotor, to within 2 dB of the value obtained through the more complicated numerical calculation involving use of computers.

The theoretical noise predictions for our test conditions were calculated based on these charts and on the measured rotor parameters. The comparison between the predictions and data are shown in the following sections.

Table 2 Test conditions

	Thrust Effect	Blade Number Effect	Advance Ratio Effect
Blade Number (B)	2	2, 3, 4, 6	2
Rotor RPM (Ω)	672	672	672
Tip Speed (V_t), in fps (m/s)	146.6 (44.7)	146.6 (44.7)	146.6 (44.7)
Tunnel Speed (U), in fps (m/s)	44 (13.4)	44 (13.4)	29.3 (8.93) 44 (13.4) 51.3 (15.6) 58.7 (17.9)
Advance Ratio (μ)	.3	.3	.2, .3, .35, .4
Pitch at Tip (θ_s), in degrees	6.9, 8.4, 10 11.5, 13	10, 7.7, 6.5, 5.3	8.2, 10, 11, 11.9
Shaft Angle (α_s), Tilt Forward, in degrees	14.5, 15.5, 16.6, 17.6, 18.6	16.6, 15, 14.1, 13.3	14.1, 16.6, 17.9, 19.1
Thrust (T), in lbs. (kg.)	2.26 (1.02) 2.73 (1.24) 3.22 (1.46) 3.54 (1.61) 3.74 (1.70)	3.22 (1.46)	3.22 (1.46)
Thrust Coefficient (C_t) $= T/\rho\pi R^2 V_t^2$	.0032, .0039, .0046, .0051, .0054	.0046	.0046
Blade Loading Coef. (C_t/σ)	.0628, .0766, .0903, .1001, .1060	.0903	.0903
Tip Path Plane Angle (α_{TPP}), in degrees	9	9	9

Thrust Effect

A two-bladed rotor of 672 rpm [$V_t = 146.6$ fps (44.7 m/s)] was used in this test. The tunnel speed was 44 fps (13.4 m/s). The shaft angle was adjusted to maintain a constant tip path angle of 9 ± 0.4 deg.

Figure 4 shows the sound pressure level (SPL) in decibels versus harmonic number m for various rotor thrust. The frequency of mth harmonic is $mB\Omega$ where B is the blade number and Ω is the rotor frequency. The error bars show the scatter of data. Six data points are included in each data bar. The typical data scatter is about 5 dB. Only those data above 100 Hz are presented (the cut-off frequency of the anechoic chamber is 160 Hz). In general, the SPL decreases as the harmonic number m increases, except for the high harmonics. The theoretical predictions are plotted as broken lines on Fig. 4. The agreement between theory and data is reasonably good for the cases $C_T = 0.0039$ ($C_T/\sigma = 0.0766$) and $C_T = 0.0051$ ($C_T/\sigma = 0.1001$). The agreement is not as good for the cases of high and low disk loading. The agreement is best for the case of $C_T/\sigma = 0.0766$, which is within the normal cruise range. The theory always underestimates some of the highest noise harmonics. The noise data is taken along the rotor axis where each frequency of the loading mode results in one acoustic frequency. In a sense, the noise spectra indicate the rotor harmonic loading. From Fig. 4, it can be seen that a single loading relation ($F_\lambda \sim \lambda^{-k}$) as used in Ref. 5 works reasonably well for the prediction of rotational noise of the middle-frequency range for the cruise mode. For the high-frequency noise prediction, another blade loading relation is probably required.

Figure 5 shows the rotational noise versus rotor thrust (disk loading) for each harmonic. The first seven harmonics are below the anechoic chamber cut-off frequency. However, as far as the comparison of the same noise harmonic (same frequency) goes, the effect of reverberation is not important.

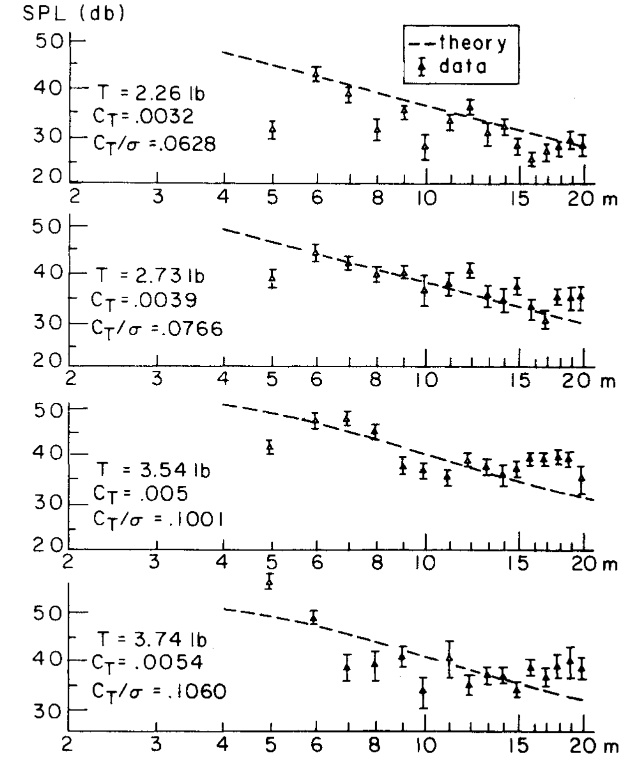

Fig. 4 The comparison of data with theory at various rotor thrust: $\mu = 0.3$, $V_t = 146.6$ fps (44.7 m/s), $\alpha_{TPP} = 9$ deg, $B = 2$.

A straight line representing T^2 dependence is drawn on each data set as a reference. The low-harmonic-noise data show trends proportional to T^2. The trends of the profile are not clear for high harmonics. As indicated in the cases of $m = 8$ and $m = 10$, the profiles cease to increase as T^2 but level off as the disk loading increases.

Blade Number Effect

In studying the effect of blade number on the noise harmonics, the tip path plane and thrust and all other parameters were kept constant. The tip path plane angle was maintained at 9 ±0.4 deg. The thrust was maintained at 3.22 ±0.2 lb (1.46±0.09 kg), corresponding to $C_T = 0.0046$. The rotor speed and tunnel speed were 672 rpm and 44 fps (13.4 m/s), respectively. The blade numbers were 2, 3, 4, and 6. The solidity was varied as the rotor blade number was changed, since only one set of blades was available. Figure 6 shows the rotor noise spectra for various blade numbers. Note that the spectra of different blade numbers are quite different, especially for four-bladed rotors. For the six-bladed rotor, the noise level of $m = 3$-7 reduces smoothly with harmonic number m. The corresponding frequency of the 7th harmonic is 42 Ω, where Ω is the rotor angular velocity. The noise harmonics of the two-bladed rotor are also reduced smoothly up to $m = 7$. However, the corresponding frequency is only 14 Ω. As seen in Fig. 6, the agreement between theory and data is good for the three and six-blade rotors. The agreement is fair for the two-bladed rotor. The theory overestimates the four-bladed rotor.

Figure 7 shows the effect of blade number B on the rotational noise. The SPL of $n = 24$ and $n = 36$ harmonics are plotted, since these are each divisible by 2, 3, 4, and 6, which correspond to the various blade numbers studied ($n = mB$). The effect of harmonic number m is corrected by subtracting $-20 \log m$ from the sound pressure level, to account for the assumed m^{-2} relation. This correction is based on the result that lines (not shown) proportional to m^{-2} roughly fit the data in Figs. 4, 6, and 8. Note that the data of harmonics of $n = 24$ and 36 collapse together after the correction. A line of SPL proportional to B^{-2} is drawn for reference. The sound pressure is proportional to the thrust generated by each blade. The thrust of each blade is inversely proportional to the blade

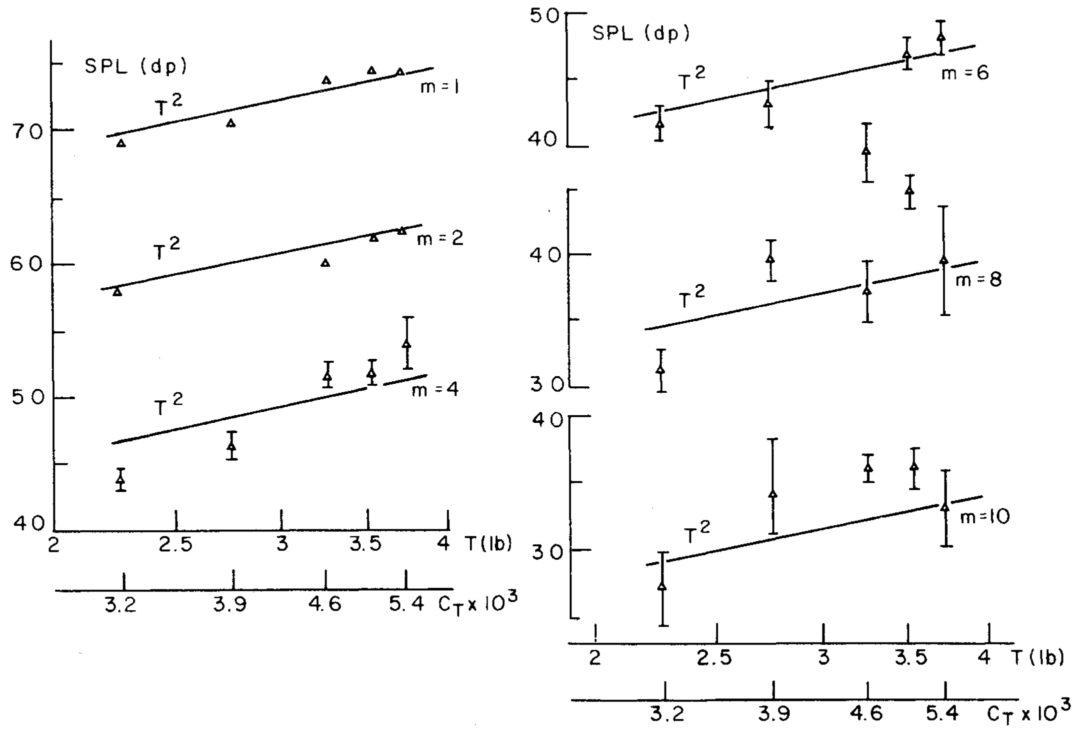

Fig. 5 The dependence of rotational noise level with thrust: $\mu = 0.3$, $V_t = 146.6$ fps (44.7 m/s), $\alpha_{TPP} = 9$ deg, $B = 2$.

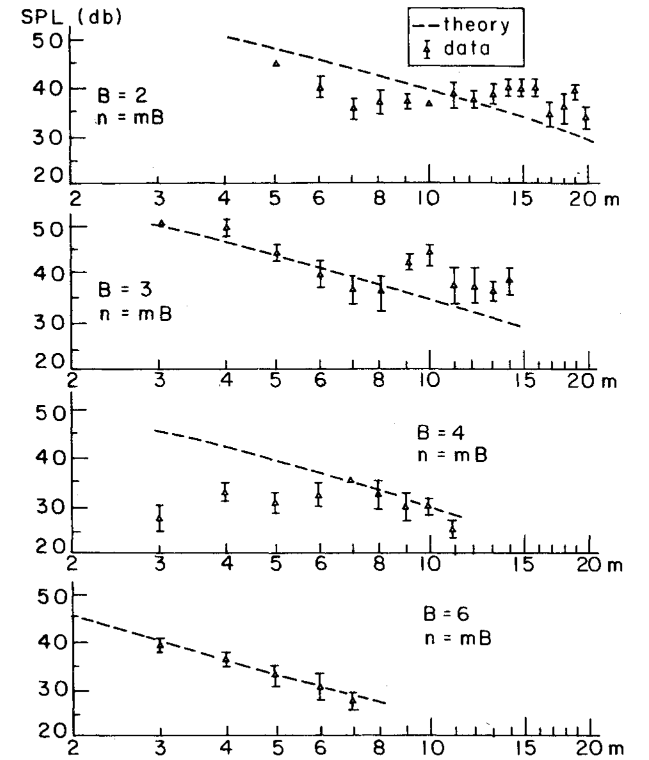

Fig. 6 The comparison of data with theory at various blade number: $T = 3.22$ lb (1.46 kg), $C_T = 0.0046$, $\mu = 0.3$, $V_t = 146.6$ fps (44.7 m/s), $\alpha_{TPP} = 9$ deg.

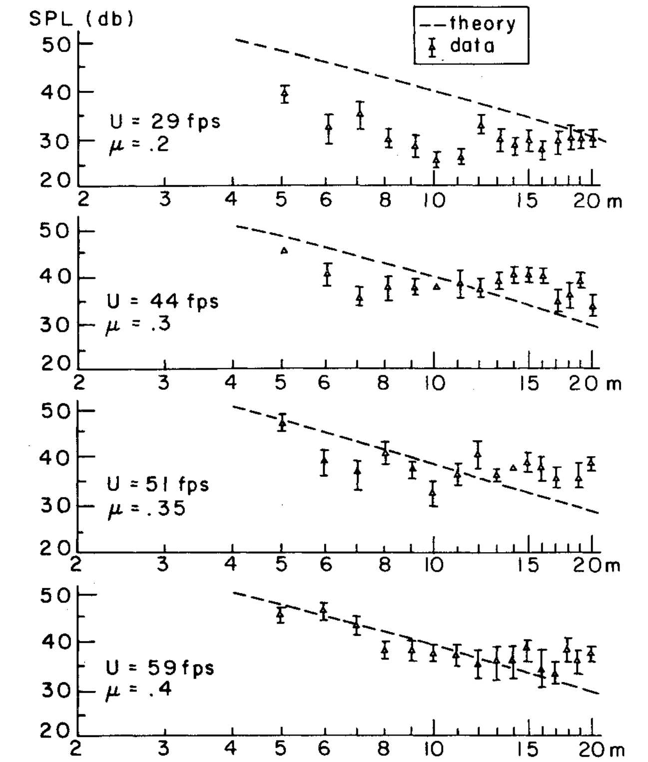

Fig. 8 The comparison of data with theory at various advance ratios: $T = 3.22$ lb (1.46 kg), $C_T = 0.0046$, $V_t = 146.6$ fps (44.7 m/s), $\alpha_{TPP} = 9$ deg, $B = 2$.

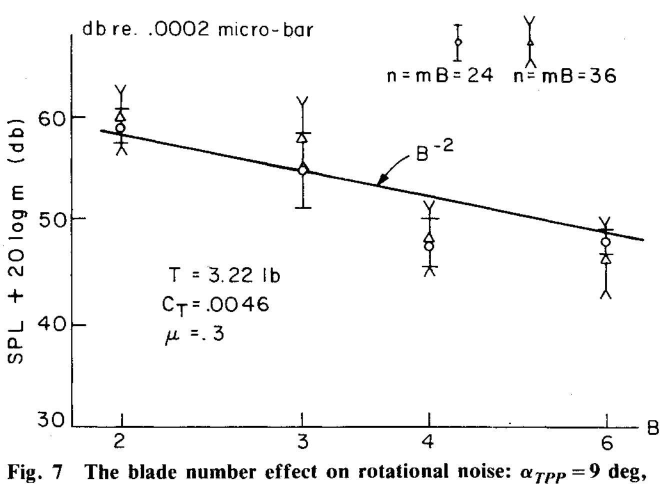

Fig. 7 The blade number effect on rotational noise: $\alpha_{TPP} = 9$ deg, $V_t = 146.6$ fps (44.7 m/s).

number B, when the total thrust is constant. The sound pressure therefore decreases as B^{-1} and sound intensity as B^{-2}. However, the change of wake structure has not been taken into account in this simple consideration. The B^{-2} proportionality fits the data reasonably well; except for the data of the four-bladed rotor. A significant reduction of noise level is obtained as the blade number is increased from three to four. The reduction is not as large when the blade number is changed from four to six.

In general, for the steady flight without blade slap, the increase in number of blades reduces the rotational noise at constant thrust.

Advance Ratio Effect

A two-bladed rotor of angular velocity of 672 rpm was used in the study of advance ratio effect on rotational noise. The tunnel wind speeds were 29, 44, 51, and 59 fps (8.93, 13.4, 15.6, and 17.9 m/s) to obtain the advance ratios (tunnel speed/tip speed) of 0.2, 0.3, 0.35, and 0.4. The thrust and tip path plane angle were kept constant; 3.22 ±0.2 lb (1.46±0.09 kg) and 9±0.4 deg, respectively.

Figure 8 shows the spectra of rotational noise for various advance ratios. The spectrum shape does not change significantly as the advance ratio changes. The theory in Ref. 5 assumes that unsteady loading does not change with advance ratio and accordingly, there should not be any change on noise level at our microphone location for different advance ratios. This is certainly not the case in reality. As seen in Fig. 8, the theory overestimates the noise levels in the case of $\mu = 0.2$. The agreement is fair for $\mu = 0.3$ and $\mu = 0.35$, and is good for $\mu = 0.4$.

Figure 9 shows the sound pressure level of various noise harmonics versus advance ratio. As would be expected, the level of the low harmonics increases with increasing forward speed due to an increasing asymmetry and unsteadiness in the loading. Lines of SPL proportional to μ^4 and μ^2 are drawn for references; the μ^4 line fits the 1st and 4th to 9th harmonic noise reasonably well. For the high harmonics, such as 10th and 11th, the noise level tends to level off at high advance ratios.

Directivity

A two-bladed rotor operating at 1100 rpm [$V_t = 240$ fps (73.1 m/s)] was used in this directivity measurement. The tunnel speed was 88 fps (26.8 m/s) ($\mu = 0.37$). The thrust (T), thrust coefficient (C_T), and blade loading coefficient (C_T/σ) were measured to be 10.6 lb (4.81 kg), 0.0057, 0.1119, respectively.

Figure 10 shows the directivity of the noise harmonics. It was measured in the plane which is normal to the tunnel axis and passing through the center of the rotor. Because of space restriction, the microphone was mounted at 53 in. (1.35 m) from the rotor as the elevation angle from the horizontal plane is larger than 45 deg and 72 in. (2.19 m) as elevation is equal or less than 45 deg. The measurements were corrected to the same distance. As seen in Fig. 10, there are dips around 20 deg above the disk plane, for the 6th-8th noise harmonic. For

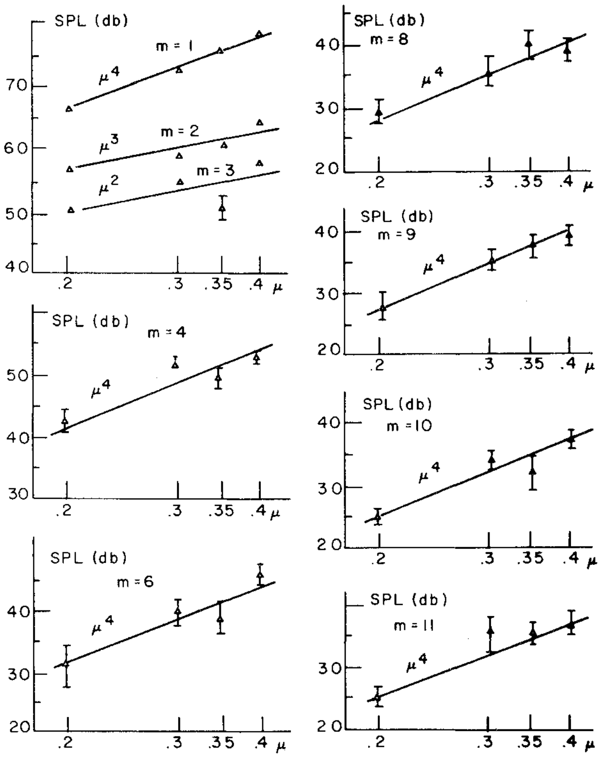

Fig. 9 The advance ratio effect on rotational noise: $T = 3.22$ lb (1.46 kg), $C_T = 0.0046$, $V_t = 146.6$ fps (44.7 m/s), $\alpha_{TPP} = 9$ deg, $B = 2$.

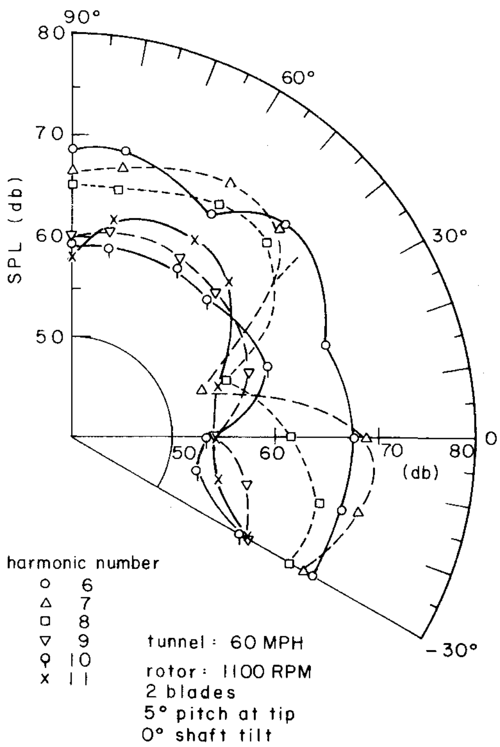

Fig. 10 Directivity of rotational noise.

the 9th-11th harmonic, dips occur near disk plane. Lowson and Ollerhead[5] found theoretically that the rotational noise directivity should have a dip slightly above the rotor disk for the low harmonics and the dip moves toward the rotor disk plane for the higher harmonics. The dip is basically due to the cancellation between thrust and drag effects on acoustic radiation above the disk. Our experimental data agree with their theoretical prediction.

V. Discussion

The rotor flowfield is very complicated. In addition to the possible blade stall at the retreating side and possible compressibility effects at the advancing side, each blade generates its own vortex wake. Mutual interactions occur between the vortex system and the blade. The induced flowfield is highly nonuniform across the rotor disk. The induced unsteady loading, in addition to the steady loading, is believed to be the main source of rotational noise. The Reynolds number and Mach number affect the vortex structure and vortex core size, in addition to stall and compressibility and hence, the unsteady loading and noise radiation. However, the exact effects are far from clear. This paper does not intend to predict the noise radiation of a full-scale helicopter from the model rotor test. The model rotor data are mainly used as a data base for the evaluation of existing helicopter noise theory and noise sources.

A question of near-field effect arises when the measurement is made within a confined environment and when a comparison with far-field predictions of Ref. 5 is made. The region around the rotor can be divided into far field, near field, and intermediate region, both acoustically and geometrically. At a distance r from the source, which is large compared with the sound wavelength, the fluid velocity is in phase with the pressure. All the energy is radiated outward with the speed of sound. This region is called acoustical far field. In contrast, in the acoustical near field, where $r \ll$ wavelength, the fluid velocity is out of phase with the pressure. This reactive energy does not radiate as sound to the far field, but microphones in the near field can sense it. The geometric far field is where $r \gg D$, where D is the rotor diameter. The sound amplitude difference due to the source distribution is negligible in the geometric far field. However, the phase difference is not negligible, unless the source is compact. The geometric near field is where $r \ll D$, and the effects caused by the distribution of the source is important.

Our microphone location is about one rotor diameter above the rotor disk. Strictly speaking, it is in the intermediate region, rather than the far field. The measured data do have some near-field effects. The question is: Is it significant? Based on the calculation of near-field terms, Lowson and Ollerhead[5] concluded that the near-field effects (both acoustic and geometric) are negligible for distances greater than two rotor diameters. The near-field effects were calculated to be approximately 3 dB at one diameter away and 10 deg below the rotor disk. The near-field effect is dependent on the relative position to the rotor disk. The minimum effect is expected to occur along the rotor axis which corresponds to our microphone location. It is believed that the data presented in this paper have a near-field effect of approximately 3 dB or less. Therefore, the data should be useful in a comparison with far-field theoretical predictions. It is not believed that the near field effect is responsible for the discrepancy between data and predictions.

The discrepancies between our data and theory is believed mainly due to the theoretical aerodynamic modeling rather than the acoustic modeling.

The assumption of airloading harmonics, $F_\lambda \propto \lambda^{-2}$, is probably a reasonable one for a range of loading harmonics. It is not expected to be valid for the whole range of harmonics, considering that it was obtained from the first ten airloading harmonic data. If different values of k are assigned for different frequency ranges and flight conditions, the accuracy of prediction may be improved. The proper value of k may be determined from the airloading data at high frequency or from a comparison between theory and acoustic measurement at proper locations, such as along the rotor axis.

The acoustic model of a point loading on the blade is applicable at our test conditions. As indicated before, the magnitude of equivalent point loading was derived based on the correlation relation $e^{-a\lambda\xi}$ along the blade. The correlation concept is useful. The problem is to select the correct value for the correlation parameter a, which is a function of flight conditions. Since no useful data were available, an arbitrary value was chosen. This may be another source of error in the theory.

The phase relations between different airloading harmonics have very significant effects on acoustic radiation. The assumed random phase in the theoretical modeling is certainly not a realistic one. However, it may be the best assumption one can make with no useful data available. Nevertheless, it is not the source of the discrepancy between our data and the theory. This is because our data were obtained along the rotor axis. There is no doppler effect at this location. One loading harmonic only produces one acoustic harmonic along the rotor axis. Therefore, the phase relationship between loadings will not affect the noise radiation.

In viewing of the comparison between data and the theory, it is felt that the main deficiency of rotor noise prediction is due to the lack of rotor aerodynamic data such as the amplitude and the phase of harmonic loading and correlation lengths along the span of the blade. The approach and the acoustic modeling of Ref. 5 are believed to be adequate for the rotor rotational noise prediction.

VI. Conclusions

The rotational noise of helicopter rotors in forward flight was studied in a controlled environment, namely an anechoic wind tunnel. The parameters under study were thrust (blade loading), blade number, and advance ratio. The separate effects of each parameter were studied with the other parameters being kept constant.

The rotational noise of low harmonics was found to be proportional to thrust squared. For high-harmonic noise, the trend is not so clear. As the blade loading increases, the high-harmonic noise tends to level off. In steady flight, increased blade number reduces the rotational noise as expected. A significant reduction of noise is obtained as the blade number is increased from three to four. The noise reduction is not as large when the blade number is changed from four to six.

As would be expected, the noise of low harmonics increases with the forward flight speed. The 1st and 4th-9th noise harmonics increase with advance ratio to a fourth power. The data of 2nd and 3rd noise harmonics fit better with the advance ratio squared. For higher harmonics, the sound levels off at high advance ratios.

The measured noise directivity shows a dip slightly above the rotor disk for low harmonic noise. The dip moves toward the rotor disk for the high harmonics. This agrees with the prediction in Ref. 5.

Twelve sets of data for rotational noise as a function of frequency have been compared with the theoretical prediction of Lowson and Ollerhead.[5] In general, the agreement is reasonably good, except for the case of 1) low and high disk loading, 2) four-bladed rotor, and 3) low advance ratio. The theory always underestimates the rotational noise at high harmonics. The result of comparison suggests that some refinements in the theory are necessary to obtain satisfactory predictions of noise level at various flight conditions.

Acknowledgment

This work was partially supported by USAMRDL/NASA Ames, Contract No. NAS2-7684.

References

[1] Cox, C. R., "Aerodynamic Sources of Rotor Noise," *Journal of the American Helicopter Society*, Vol. 18, Jan. 1973, pp. 3-9.

[2] Gutin, L. Ya., "On the Sound Field of a Rotating Propeller," NACA TM-1195, Oct. 1948.

[3] Schlegel, R. G., King, R. J., and Mull, H. R., "Helicopter Rotor Noise Generation and Propagation," USAAVLABS TR 66-4, Fort Eustis, Va., Oct. 1966.

[4] Schlegel, R. G. and Bausch, W. E., "Helicopter Rotor Noise Prediction and Control," *Journal of the American Helicopter Society*, Vol. 14, July 1969, pp. 38-47.

[5] Lowson, M. V. and Ollerhead, J. B., "Studies of Helicopter Rotor Noise," USAAVLABS TR 68-60, Fort Eustis, Va., Jan. 1969.

[6] Sadler, S. G. and Loewy, R. G., "A Theory for Predicting the Rotational and Vortex Noise of Lifting Rotors in Hover and Forward Flight," NASA CR 1333, May 1969.

[7] Wright, S. E., "Sound Radiation from a Lifting Rotor Generated by Asymmetric Disk Loading," *Journal of Sound Vibration*, Vol. 9, March 1969, pp. 223-240.

[8] Wright, S. E., "Discrete Radiation from Rotating Periodic Sources," *Journal of Sound Vibration*, Vol. 17, Aug. 1971, pp. 437-498.

[9] Scheiman, J., "A Tabulation of Helicopter Rotor-Blade Differential Pressures, Stresses, and Motions, as Measured in Flight," NASA TM-X-952, March 1964.

[10] Boxwell, D. A., Schmitz, F. H., and Hanks, M. L., "In-Flight Far Field Measurement of Helicopter Impulsive Noise," First European Rotorcraft and Powered Lift Aircraft Forum, Southampton, England, Sept. 22-24, 1975.

[11] Cox, C. R., "Rotor Noise Measurements in Wind Tunnel," *Proceedings of the Third CAL/AVLABS Symposium*, Buffalo, New York, June 18-20, 1969.

[12] Bauer, P. and Widnall, S. E., "The Development of a Wind Tunnel Facility for the Study of V/STOL Noise," MIT, Cambridge, Mass., FTL Rept. R-72-6, Aug. 1972.

[13] Harris, W. L. and Lee, A., "The Development of Experimental Techniques for the Study of Helicopter Rotor Noise," AIAA Paper 75-455, Hampton, Va., March 1975.